

See discussions, stats, and author profiles for this publication at: <https://www.researchgate.net/publication/280998957>

Coverage Dependence of Methanol Dissociation on TiO₂(110)

ARTICLE *in* JOURNAL OF PHYSICAL CHEMISTRY LETTERS · AUGUST 2015

Impact Factor: 7.46 · DOI: 10.1021/acs.jpclett.5b01417 · Source: PubMed

CITATIONS

2

READS

55

7 AUTHORS, INCLUDING:



Bo Wen

Beijing Computational Science Research Center

8 PUBLICATIONS 26 CITATIONS

[SEE PROFILE](#)



Chuanyao Zhou

Dalian Institute of Chemical Physics

14 PUBLICATIONS 129 CITATIONS

[SEE PROFILE](#)



Li-Min Liu

Beijing Computational Science Research Center

101 PUBLICATIONS 1,062 CITATIONS

[SEE PROFILE](#)



Zefeng Ren

Peking University

28 PUBLICATIONS 697 CITATIONS

[SEE PROFILE](#)

Coverage Dependence of Methanol Dissociation on TiO₂(110)

Shuo Liu,^{†,‡,§,||} An-an Liu,^{†,‡,§,||} Bo Wen,^{†,‡,§,||} Ruidan Zhang,^{†,||} Chuanyao Zhou,[§] Li-Min Liu,^{*,‡} and Zefeng Ren^{*,†,||}

[†]International Center for Quantum Materials (ICQM) and School of Physics, Peking University, Beijing 100871, P. R. China

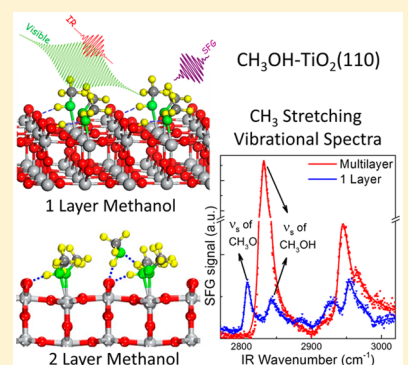
[‡]Beijing Computational Science Research Center, Beijing 100094, P. R. China

[§]State Key Laboratory of Molecular Reaction Dynamics, Dalian Institute of Chemical Physics, Chinese Academy of Sciences, 457 Zhongshan Road, Dalian 116023, Liaoning, P. R. China

^{||}Collaborative Innovation Center of Quantum Matter, Beijing 100871, P. R. China

Supporting Information

ABSTRACT: Although the photochemistry of methanol on TiO₂(110) has been widely investigated as a prototypical model of the photocatalytic reaction of organic molecules, the most fundamental question of the adsorption state of methanol on TiO₂(110) is still unclear. We have investigated the adsorption of methanol on TiO₂(110) using sum frequency generation vibrational spectroscopy (SFG-VS) and density functional theory (DFT) calculations. The SFG results indicate the dissociation of methanol is highly dependent on the coverage. The DFT calculations suggest that the methanol prefers the partially dissociated structure at low coverage, whereas the second layer methanol, which is hydrogen-bonded to the bridge-bonded oxygen site, largely blocks the dissociation of the first layer methanol. Our results not only resolves a long-standing debate regarding the adsorption state of methanol on TiO₂(110) but also provides a detailed insight into the adsorption structure and sheds light on the photochemistry on this surface at the molecular level.



Titanium dioxide, TiO₂, has been extensively studied as a promising photocatalyst in wide range of applications including photosplitting of water and photooxidation of organic molecules,^{1–5} ever since the first report of ultraviolet-induced redox chemistry on TiO₂ surfaces.⁶ The photochemistry of methanol on TiO₂ surfaces has been widely investigated because methanol acts as a hole scavenger to facilitate water splitting.⁷ The simplest alcohol, methanol, on TiO₂ surfaces is often considered as a prototype for the photocatalytic oxidation of organic molecules.^{5,8,9} In particular, the most stable surface, rutile TiO₂(110), has been highly investigated as a model for fundamental studies of TiO₂ at the molecular level.^{8,9} However, the most fundamental question of the adsorption state of methanol on TiO₂(110), whether dissociative or molecular, has not been answered satisfactorily to date either experimentally^{10–23} or theoretically.^{18,24–30}

Recently, the adsorption and reactions of methanol on TiO₂(110) have been extensively studied.^{16–18,20–23,31–37} The most common defects on the surface of reduced TiO₂(110) are bridge-bonded oxygen (O_{br}) vacancies (see Figure 1). Previous experiments have confirmed that methanol dissociatively adsorbs on the vacancies, forming bridging methoxy (CH₃O_{br}) and hydroxyl groups (HO_{br}).^{12,17} However, on five coordinated titanium (Ti_{5c}) sites, the adsorption state is still controversial. Scanning tunneling microscopy (STM) studies suggest that methanol is intact on Ti_{5c} sites.^{17,18} In other studies, molecular methanol was considered to undergo photoinduced dissociation to methoxy through the breaking

of the O–H bond,^{18,21,33} and then further photooxidized into formaldehyde and methyl formate.^{22,23,33,34} Thus, a stepwise breaking of C–H bond, or stepwise photooxidation of methoxy was suggested. However, methoxy was identified to be a photoactive species, whereas the molecularly adsorbed methanol was considered to be photoinactive.^{20,31,32} Additionally, it was proposed that methoxy on Ti_{5c} sites is formed only by the thermal dissociation of methanol on TiO₂(110), initiated by defects, coadsorbed oxygen adatoms, or terminal OH groups.^{20,31,32} Because alcohol decomposition is often used to identify catalytically active sites on metal oxide surfaces in single crystalline and powder form,⁸ it is essential to identify the adsorption state of methanol on TiO₂(110), as this would provide a fundamental understanding into this prototypical system, as well as important insights into surface photocatalytic reactions.

Vibrational spectroscopy is a powerful tool to investigate the chemical identity, structure, kinetics, and dynamics of adsorbates on surfaces.³⁸ Due to the damaging effect of electrons and photons (ultraviolet and X-ray) on the adsorbates, studying the adsorption state should be always careful and involve methods that are mild and nondestructive. Infrared (IR) spectroscopy, which is routinely used for vibrational studies of molecules on surfaces, has been largely

Received: July 5, 2015

Accepted: August 7, 2015

Published: August 7, 2015



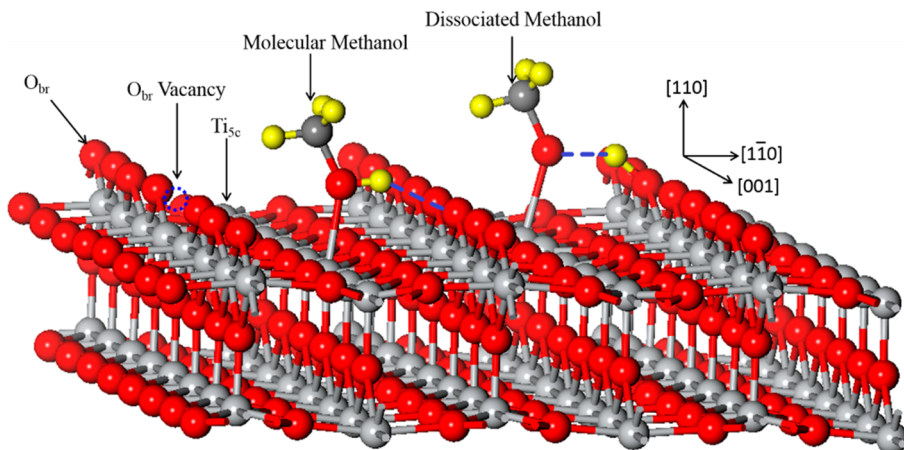


Figure 1. $\text{TiO}_2(110)$ surface model showing the bridge-bonded oxygen (O_{br}) vacancy, and the molecular and dissociated methanol adsorbed on five-coordinated Ti (Ti_{sc}) sites.

applied to thin films and metal surfaces. However, single crystal oxide surfaces present a problem because of their minimal reflectivity.^{39,40} Sum frequency generation vibrational spectroscopy (SFG-VS), as a surface and interface specific tool, has been used successfully to probe the molecular composition, interactions, as well as the orientational and conformational structures of surfaces and interfaces.^{41–43} Methanol adsorption on TiO_2 particles and thin films has been investigated by both IR spectroscopy and SFG, and both molecular and dissociative methanol adsorption states have been observed.^{44–47} However, those samples have uncharacterized surfaces that precluded a detailed investigation of the adsorption sites and structures.

In an effort to elucidate the methanol adsorption state on $\text{TiO}_2(110)$, we have conducted the SFG-VS measurements and DFT calculations. Our experiments resolved both the molecularly and dissociatively adsorbed methanol, namely the methoxy, on Ti_{sc} sites, and they also show that the adsorption state of methanol is greatly affected by the coverage. At no more than one layer, both methanol and methoxy forms can coexist on Ti_{sc} sites, which corresponds to a partially dissociated structure. When the second layer appears, the fraction of methoxy gradually decreases and even disappears at multilayer coverage. The coverage-dependent percentage of methoxy has also been quantitatively estimated at different coverages. Our results not only settle the long-standing debate of the methanol adsorption state, but also provide new insight into the multilayer structure of methanol and the photochemistry on $\text{TiO}_2(110)$.

Figure 2 shows the SFG vibrational spectra in the C–H stretching region from methanol of no more than one layer coverage on the $\text{TiO}_2(110)$ surface for the *ssp* polarization combination (SF output, visible input, and IR input are *s*, *s*, and *p* polarized, respectively). Methanol was overdosed at 120 K, and different coverages were achieved by flashing the substrate at 200, 240, 260, and 280 K. Four major resonant peaks were clearly resolved. To exclude the possible effect of the flashing temperature on the methanol adsorption state, methanol was dosed by backfilling the chamber at 120 K and the SFG spectra were found to show almost the same features. A fit of the SFG spectra for one layer methanol, prepared by flashing at 200 K,¹² gives vibrational resonances at 2807.1, 2840.5, 2920.4, and 2950.8 cm^{-1} (see Table S1, Supporting Information). From the studies on TiO_2 thin film,^{46,47} the resonant frequencies at 2807.1 and 2840.5 cm^{-1} can be attributed to the symmetric (ν_s)

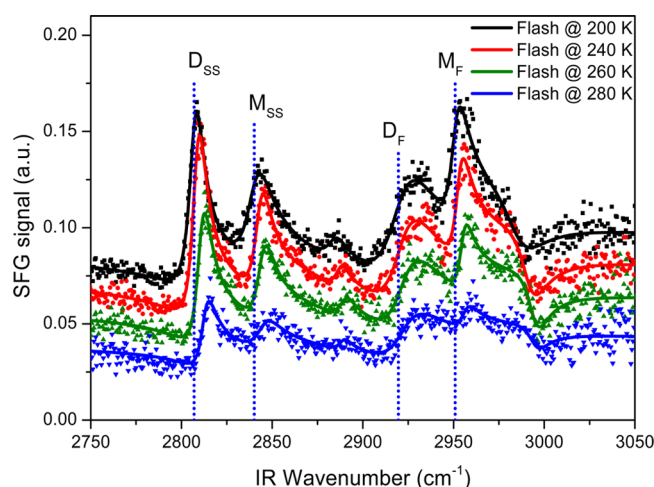


Figure 2. SFG vibrational spectra (*ssp* polarization combination) of CH_3OH with different coverages on $\text{TiO}_2(110)$ by overdosing at 120 K and flashing at 200, 240, 260, 280 K. The coverage by flashing at 200 K corresponds to the full first layer. Dotted and solid lines are experimental data and fitting results, respectively. The vertical dotted lines indicate four resonant frequencies of one layer coverage: 2807.0, 2840.2, 2919.6, and 2950.9 cm^{-1} . Spectra are offset vertically by 0.02 sequentially for clarity. Methanol can adsorb on the TiO_2 surface both in molecular form (CH_3OH) and dissociated form (CH_3O), which are indicated by “M” and “D” correspondingly. The subscripts “ss” and “F” stand for the symmetric stretching mode and Fermi resonance of CH_3 group, respectively.

CH_3 stretching vibration of the dissociatively adsorbed methanol, methoxy, on Ti_{sc} sites ($\text{CH}_3\text{O}-\text{Ti}_{\text{sc}}$) and the molecularly adsorbed methanol at Ti_{sc} sites ($\text{CH}_3\text{OH}-\text{Ti}_{\text{sc}}$), respectively. The resonances at 2920.4 and 2950.8 cm^{-1} are from the $\text{CH}_3\text{O}-\text{Ti}_{\text{sc}}$ and $\text{CH}_3\text{OH}-\text{Ti}_{\text{sc}}$, respectively. These resonances can be assigned to the Fermi resonance of the CH_3 ν_s mode with overtones of the CH_3 bending mode based on SFG spectra of the pure liquid methanol/air interface.^{48,49} The fitting shows that the peak width of the resonance at 2920 cm^{-1} is much larger than other peaks. A possible reason could be that another Fermi resonance of $\text{CH}_3\text{OH}-\text{Ti}_{\text{sc}}$ may partially overlap with the Fermi resonance of $\text{CH}_3\text{O}-\text{Ti}_{\text{sc}}$. All the resonant frequencies are found to be blue-shifted by 4–6 cm^{-1} as the methanol coverage decreases. There is a small bump at around 2890 cm^{-1} , which is tentatively assigned to another Fermi

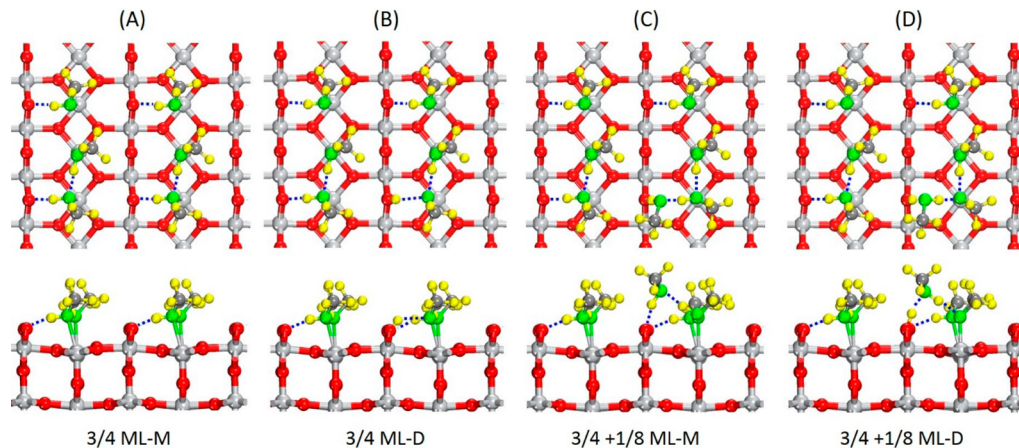


Figure 3. Top and side views of optimized molecular and dissociated adsorption of 3/4 ML methanol in the first layer (A and B) or those with additional 1/8 ML in the second layer (C and D) on the 4 × 2 $\text{TiO}_2(110)$ surface unit cell. “M” and “D” represent molecular and dissociative adsorptions, respectively. Blue dashed lines show hydrogen bonds.

resonance of $\text{CH}_3\text{O}-\text{Ti}_{5c}$.^{48,49} A feature at 2989 cm^{-1} can be resolved, which is probably from the antisymmetric (ν_{as}) CH_3 stretching mode of $\text{CH}_3\text{O}-\text{Ti}_{5c}$ or $\text{CH}_3\text{OH}-\text{Ti}_{5c}$. More detailed assignments for the overlapping Fermi resonance and the antisymmetric stretching mode would need more polarization-dependent and high-resolution measurements. The nonresonant signal, corresponding to the baseline away from resonance peaks, was found to increase as the coverage of methanol was reduced (see Supporting Information Figure S2 and Table S1). This may be due to the influence of adsorbed molecules on the surface electronic state of $\text{TiO}_2(110)$.⁵⁰

For spectroscopic studies on single crystal TiO_2 , the most detailed results are from high-resolution electron energy loss spectroscopy (HREELS) on $\text{TiO}_2(110)$.¹² The HREELS has limited resolution and could not resolve the methoxy and methanol resonances in the C–H stretching region. The feature at 3660 cm^{-1} corresponding to a surface hydroxyl group suggests a possible methanol dissociation to methoxy, but it also possibly originates from electron-induced decomposition.¹⁰ However, the vibrational spectra obtained in this study allow us to reach an unambiguous conclusion that both molecular and dissociative states of methanol coexist on $\text{TiO}_2(110)$.

In order to determine the adsorption state at different coverages of methanol, DFT calculations were performed on defect-free $\text{TiO}_2(110)$. To determine the coverage effect on the adsorption states, different adsorption structures with a series of coverages (1/8 monolayer (ML), 1/4 ML, 1/2 ML, 3/4, and 1 ML) have been systematically calculated. Calculated results in Supporting Information Figure S4 show the relation of the average methanol-surface distance and the n th adsorption energy to the methanol coverage. Additional methanol over 3/4 ML to form 1 ML has a longer distance from the surface by more than 0.4 Å and a lower adsorption energy by about 0.16 eV. However, adding this additional methanol to the second layer leads to a more stable structure than forming a 1 ML coverage by about 0.14 eV. The main reason for this is the strong steric hindrance between methyl groups, which repels further methanol adsorption in the first layer over 3/4 ML coverage. The structure of 3/4 ML methanol on $\text{TiO}_2(110)$ shows that a hydrogen bond (HB, dashed line in Figure 3A) is formed intermolecularly as well as between the methanol molecules and O_{br} atoms, which largely increases the adsorption energy.²⁸ The 3/4 ML methanol on $\text{TiO}_2(110)$ in

the first layer is in good agreement with a recently reported absolute coverage measurement.¹⁹

After determining that the maximum coverage of the first layer is 3/4 ML, we proceeded to explore the stable adsorption states of methanol. Both molecular and the possible dissociative adsorption states on Ti_{5c} sites were thoroughly considered by DFT calculations (see Supporting Information Figure S5). Supporting Information Table S2 and Figure S5 summarize the calculated adsorption energies for the different configurations of molecular and dissociative adsorption of 3/4 ML methanol on $\text{TiO}_2(110)$. The adsorption energy of the molecular state is 0.57 eV, and that of the partially dissociated structure with 1/6 and 1/3 methanol dissociated is 0.55 eV. Thus, these two states are almost the same. Hence, we expect that both molecular and dissociative states can coexist as shown in the above experiment and previous theoretical work.^{18,24–29} Further, we also calculated the reaction barriers of methanol dissociation for 1/8 and 3/4 ML coverages (see Figure 6), and the corresponding barriers were found to be within 0.2 eV, which is also consistent with previous results.^{27,33}

As the methanol coverage increases from one layer to multilayer, the SFG vibrational spectra dramatically change (see Figure 4). By flashing the substrate to 160 K to desorb the multilayer and part of second layer, the SFG ν_s peak of $\text{CH}_3\text{O}-\text{Ti}_{5c}$ is smaller than that for one layer coverage (green in Figure 4), whereas that for $\text{CH}_3\text{OH}-\text{Ti}_{5c}$ is larger. By flashing to 150 K to increase the second layer coverage, the methoxy peak becomes even smaller, whereas the methanol peak is further increased. Furthermore, the methoxy feature completely disappears for multilayer coverage, achieved by flashing at 140 K. We excluded the temperature effect again: by overdosing methanol at 120 K, flashing at 200 K, then dosing methanol by backfilling the chamber at 120 K. It was also observed that the ν_s feature of $\text{CH}_3\text{O}-\text{Ti}_{5c}$ became smaller or vanished. Additionally, the ν_s resonant frequency of molecularly adsorbed methanol is gradually red-shifted from one layer to multilayer, and merges to 2831.3 cm^{-1} , which is close to the resonance of the amorphous solid methanol.⁵¹ The ν_s peak of $\text{CH}_3\text{OH}-\text{Ti}_{5c}$ for 1–2 layers is much wider than that for ≤ 1 layer, which is due to the different resonances for the first and second layers. For multilayer coverage, there is a small shoulder at about 2920 cm^{-1} , attributed to another Fermi resonance, which is similar to the liquid methanol/air SFG spectra.⁴⁸ The

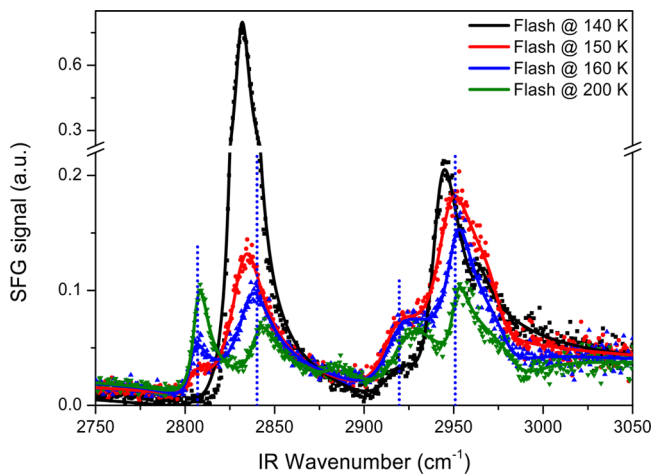


Figure 4. SFG vibrational spectra (ssp polarization combination) of CH_3OH on $\text{TiO}_2(110)$ for more than one-layer coverage by overdosing at 120 K and flashing at 140, 150, and 160 K. Dotted and solid lines are experimental data and fitting results, respectively. The vertical dotted lines indicate four resonant frequencies of one-layer coverage.

overlap of resonances from the first layer, second layer and multilayer makes a reasonable fitting impossible. It may be speculated that the decrease and disappearance of the ν_s peak of $\text{CH}_3\text{O}-\text{Ti}_{5c}$ could be caused by interference due to the increasing ν_s peak of $\text{CH}_3\text{O}-\text{Ti}_{5c}$. However, our simulation of

SFG spectra excluded this possibility. Moreover, the feature at about 2890 cm^{-1} , corresponding to Fermi resonance of $\text{CH}_3\text{O}-\text{Ti}_{5c}$ also diminishes and finally disappears when the coverage reaches two-layer and multilayer (see Figure 4 and Supporting Information Figure S3). The baselines show that the nonresonant signal decreases as the methanol coverage increases on the surface. The peak intensity for $\text{CH}_3 \nu_s$ largely increases from one layer to multilayer, whereas the increment of the Fermi resonance intensity is much less. This might be ascribed to the complex Fermi-resonance interaction between the symmetric stretching and the bending-motion overtone.^{52–54}

The multilayer adsorption on surfaces is a good model for liquid–solid interface.^{55,56} However, only a few experimental and theoretical studies have been done on the adsorption structures of multilayer methanol on $\text{TiO}_2(110)$.^{12,57} In addition to the TPD measurements which show the desorption temperature peak at 165 K for the second layer,^{12,19} HREELS studies show a strong hydrogen bond peak at 3245 cm^{-1} for multilayer coverage, but no additional feature in the C–H stretching region compared to the single layer coverage.¹² Our results show a strong coverage-dependence of the methanol adsorption state as the dissociation of the first layer methanol into methoxy is inhibited by the second layer, thus providing new insight into the adsorption structures on $\text{TiO}_2(110)$.

To gain more detailed adsorption structures of methanol on $\text{TiO}_2(110)$, the two-layer structure was further calculated with 1/8 ML coverage in the second layer and 3/4 ML in the first

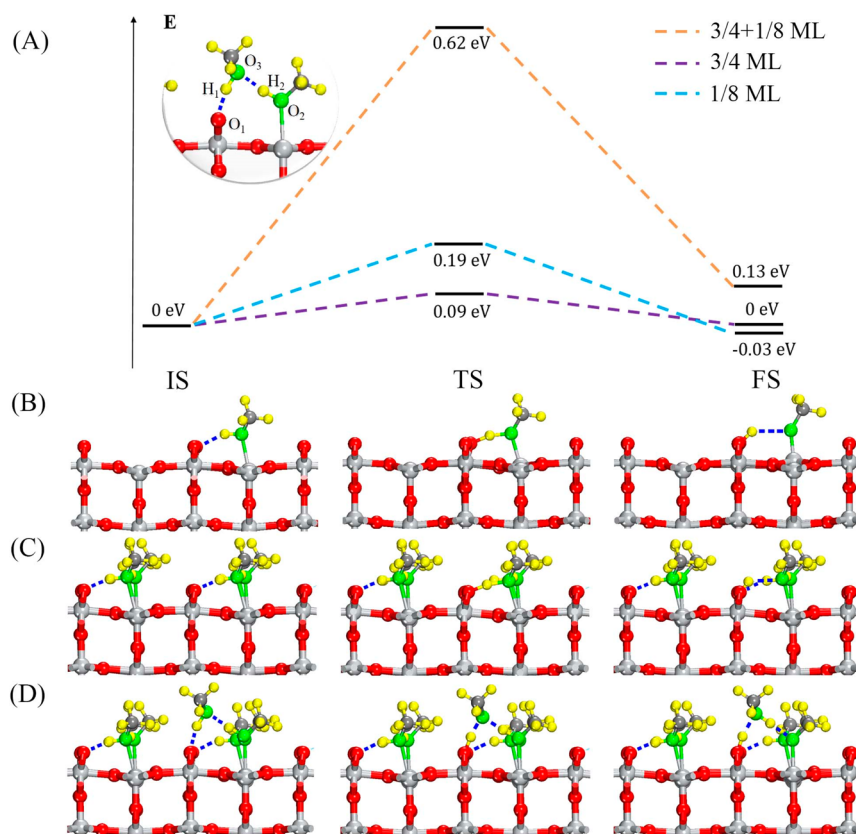


Figure 5. Potential energy profiles (A), optimized initial states (IS), transition states (TS) from the minimum energy path and final states (FS) for methanol coverages of 1/8 ML (cyan, B), 3/4 ML (purple, C), and 3/4 + 1/8 ML (orange, D). The potential energies for all the initial states potential energies are rescaled as 0 eV. The image in the circle is a magnification of the local structure for 3/4 + 1/8 ML. Blue dashed lines indicate hydrogen bonds.

layer, as shown in Figure 3C. Similar to the structure of water on $\text{TiO}_2(110)$,⁵⁸ the second layer methanol bonds to O_{br} sites ($\text{CH}_3\text{OH}-\text{O}_{\text{br}}$) via a HB, which results in the breaking of the HB between $\text{CH}_3\text{OH}-\text{Ti}_{\text{Sc}}$ and O_{br} , and the formation of a new HB between $\text{CH}_3\text{OH}-\text{O}_{\text{br}}$ and $\text{CH}_3\text{OH}-\text{Ti}_{\text{Sc}}$. If this $\text{CH}_3\text{OH}-\text{Ti}_{\text{Sc}}$ is dissociated into $\text{CH}_3\text{O}-\text{Ti}_{\text{Sc}}$ and HO_{br} (see Figure 3D), the H atom of the second layer methanol points to the O of $\text{CH}_3\text{O}-\text{Ti}_{\text{Sc}}$ to form a HB, and another HB is formed between HO_{br} and the second layer methanol. This dissociative structure lower the adsorption energy by 0.13 eV, and the dissociation barrier is 0.62 eV (see Figure 5A and 5D), which is significantly greater than the barrier for 3/4 ML. The less stable structure and the high dissociation barrier results in the preference of the first layer methanol over the methanol molecular state. In order to determine the detailed adsorption state of methanol during the growth process, methanol was placed at different sites on the surface and the adsorption states were examined. Interestingly, the methanol of the second layer showed a disinclination to adsorb beside the dissociated methanol (less stable by 0.13 eV), with the methanol layers growing only beside the molecular methanol. Thus, the initial state of methanol underneath the second layer should be the molecular state. However, for the two-layer coverage, the reverse barrier (~0.5 eV) from the partially dissociated structure (see Figure 3D) to the molecular structure (see Figure 3C) is still too high to allow conversion to the molecular structure under our experimental conditions. Due to the similar adsorption energies of the molecular and partially dissociated structures and their low interconversion barriers in the first layer, the dissociated state is in dynamic equilibrium with the molecular state. Thus, when the second layer methanol lands on the surface, it adsorbs on the O_{br} site beside the first layer methanol in the molecular state. Once the second layer methanol adsorbs, the molecular methanol in the first layer cannot convert to the dissociated state due to the high barrier.

Although the theoretical calculation agrees well with the experimental results, the calculation was based on a defect-free surface, whereas the experimental surface had $\text{CH}_3\text{O}_{\text{br}}$ and HO_{br} with concentrations of ~0.04 ML, respectively, due to dissociative adsorption of methanol on O_{br} sites. In the vicinity of $\text{CH}_3\text{O}_{\text{br}}$ and HO_{br} , the methanol on Ti_{Sc} sites presumably do not have the same structures as those calculated for the defect-free surface. However, the calculation results are believed to represent the main structure of methanol adsorbed on Ti_{Sc} sites of $\text{TiO}_2(110)$. To precisely treat the defect on $\text{TiO}_2(110)$ requires a higher level of theory at significant computational expense.⁵⁸ However, correct treatments of defects as well as induced excess charges on surfaces are critical for the calculations on defective surfaces.⁵⁹ For both theory and experiment, the influence of defects on the adsorption and photochemistry will need to be addressed in future work.

We performed a quantitative analysis of the relative number densities of $\text{CH}_3\text{O}-\text{Ti}_{\text{Sc}}$ and $\text{CH}_3\text{OH}-\text{Ti}_{\text{Sc}}$ from the fitting results. It should be noted that the SFG signal is strongly related to the orientation of surface adsorbates,⁶⁰ including the polar angle θ , and the azimuth angle φ (generally the twist angle ψ of CH_3 group along its C_{3v} axis is not accounted for in modes for ν_s symmetry consideration), where θ is the angle of the C_{3v} symmetry axis of the CH_3 group relative to the surface normal, and φ is the angle between the projection of the C_{3v} symmetry axis onto the surface and the Ti_{Sc} row. The optimized configurations for both $\text{CH}_3\text{O}-\text{Ti}_{\text{Sc}}$ and $\text{CH}_3\text{OH}-\text{Ti}_{\text{Sc}}$ at one layer coverage are listed in Supporting Information Table S3,

which shows that the CH_3 orientation is not sensitive to the adsorption state of methanol. Further analysis shows that the *ssp* SFG signal for the $\text{CH}_3 \nu_s$ modes is not related to φ when the crystal orientation [001] is at 45° relative to the plane of light incidence.⁶¹ A simulation of SFG signal as a function of the polar angle θ is plotted in Supporting Information Figure S6, which shows that the change of the SFG signal is within ±20% for θ ranging from 42° to 51° (see Supporting Information Table S3). In addition, given that the IR and Raman transition moments of the methyl group from $\text{CH}_3\text{O}-\text{Ti}_{\text{Sc}}$ and $\text{CH}_3\text{OH}-\text{Ti}_{\text{Sc}}$ were the same, their number densities and the proportion of $\text{CH}_3\text{O}-\text{Ti}_{\text{Sc}}$ can be obtained based on the Supporting Information equations S1 and S2. Figure 6

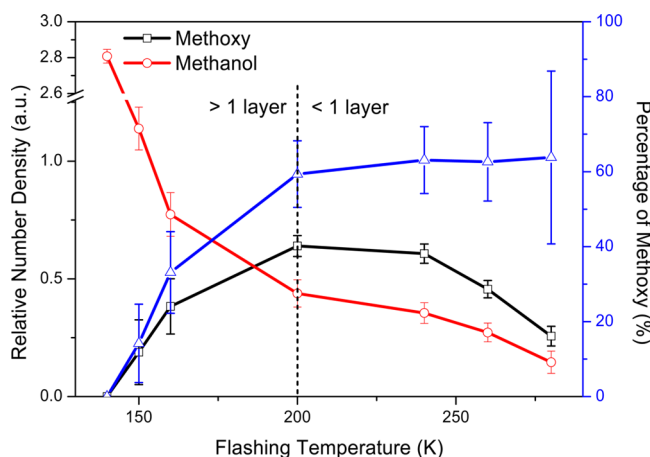


Figure 6. Relative number densities (left *y* axis, black) of methoxy (black) and methanol (red) from the fitting results of CH_3 symmetric stretching mode, and the percentage of methoxy (right *y* axis, blue) versus methanol coverages from submonolayer to multilayer on surfaces achieved by overdosing methanol and flashing the substrate at different temperatures. A full first layer corresponds to the flashing temperature at 200 K.

shows the percentage of $\text{CH}_3\text{O}-\text{Ti}_{\text{Sc}}$ is about 60% at one layer coverage without considering the orientation of the CH_3 group. The percentage of $\text{CH}_3\text{O}-\text{Ti}_{\text{Sc}}$ stayed at around 60% as the methanol coverage was reduced, whereas it decreased to zero as the coverage increased to multilayer. Although some assumptions and approximations were adopted for estimating number densities of methoxy and methanol, two valid conclusions can still be drawn: (1) the fractions of adsorbed methoxy and methanol are comparable at one layer and below and (2) the fraction of adsorbed methoxy is reduced by the second layer methanol.

The observation that the second layer methanol, hydrogen-bonded to O_{br} sites, suppresses the dissociation of the first layer methanol to methoxy on $\text{TiO}_2(110)$, is consistent with a previous report that water binding to O_{br} sites inhibits $\text{CH}_3\text{O}-\text{Ti}_{\text{Sc}}$ photodecomposition to formaldehyde.³² In other words, O_{br} sites can be occupied by a second layer of water, methanol or other alcohol molecules via HB, which will result in the O_{br} sites being unable to accept any proton from either the breaking of the O–H bond or C–H bonds of methanol or other alcohols. Hence, it can be expected that two-layer or multilayer alcohol adsorption on $\text{TiO}_2(110)$ would largely reduce the photocatalytic reactivity. However, our results only show how the second layer or multilayer methanol affect the first layer methanol dissociation at low temperature and under

ultrahigh vacuum conditions. In realistic conditions, the entropic effect relating to temperature and pressure cannot be ignored and further work in this area will likely reveal information for a more general scenario. Nonetheless, the results from this work shed light on adsorption structures and photocatalytic reactions of methanol on $\text{TiO}_2(110)$ under realistic environments.

In summary, SFG-VS and DFT calculation have been utilized to investigate the adsorption states of methanol on $\text{TiO}_2(110)$. We clearly resolved both molecularly and dissociatively adsorbed forms of methanol on Ti_{5c} sites in the C–H stretching vibration range, which suggests that methanol partially dissociates to methoxy spontaneously on this surface. For no more than one-layer coverage, comparable fractions of adsorbed methoxy and methanol coexist on Ti_{5c} sites. Furthermore, the dissociation of the first layer methanol is gradually suppressed with the increasing adsorption of the second layer, and eventually disappears at the multilayer coverage, indicating a strong coverage-dependence on the preferred adsorbed state. In particular, the dissociation of alcohol to alkoxy is the first step in the catalytic reaction of alcohol on oxide surfaces.⁸ Therefore, the hindrance of the second layer methanol to the decomposition of first layer methanol results in low photocatalytic reactivity for multilayer adsorption on $\text{TiO}_2(110)$. These results resolve a long-standing debate of the methanol adsorption state on $\text{TiO}_2(110)$ and also provide new detailed insights into the adsorption structure and help to better understand the photochemistry of organic molecules on this important surface at the molecular level.

■ EXPERIMENTAL AND COMPUTATIONAL METHODS

All SFG measurements were conducted in a compact ultrahigh vacuum (UHV) chamber with a base pressure less than 2×10^{-9} Torr.⁶² Main residual gas is H_2 due to low pumping speed for H_2 by the turbo molecular pump (80 L/s, HiPace 80, Pfeiffer). Other residual gas (like H_2O , CO, and CO_2) can get very low pressure because the cryostat with large surface area is a large cryopump when we cooled down the sample with liquid nitrogen. Commercial rutile $\text{TiO}_2(110)$ single crystal (Princeton Scientific) was fixed on a homemade sample holder with crystal orientation [001] at 45° relative to the plane of light incidence. Sample preparation was done by cycles of 500 eV Ar^+ ion sputtering and UHV annealing at 850 K. After this preparation procedure, an oxygen vacancy population of ~4% remained on the surface.³³ Methanol (99.95% purity) was further purified by several freeze–pump–thaw cycles before experiment. The surface was overdosed with methanol at 120 K. The coverage of methanol on $\text{TiO}_2(110)$ was varied by over dosing methanol at 120 K and flashing the substrate at different temperatures according to the previous TPD results.¹² One layer coverage was obtained by flashing at 200 K; one to two layers were obtained by flashing to 150 and 160 K; and multilayer coverage was obtained by flashing to 140 K. All SFG measurements were performed at 100 K. The $\text{TiO}_2(110)$ sample was situated 5 mm from a CaF_2 window.

The optical system of SFG-VS has been introduced recently.⁴⁷ The regenerative amplifier (Spitfire Ace, Spectra-Physics) delivered 35 fs pulses with a pulse energy of 5 mJ per pulse at a repetition rate of 1 kHz at the central wavelength of 800 nm. About 3 mJ was used to pump an optical parametric amplifier (TOPAS-C, Light Conversion), which generated the signal and idler pulses. The signal and idler pulses were used to

generate a tunable IR (2.6–9 μm) in a silver gallium disulfide (AgGaS_2) crystal by a noncollinear difference frequency generator (NDFG1, Light Conversion). The central wavelength used in this work was ~3.4 μm with an apparent spectral bandwidth of ~300 cm^{-1} full-width at half-maximum (fwhm) and a power of 20 mW measured before the CaF_2 window. About 1 mJ of 800 nm pulses was spectrally narrowed as the visible light (VIS) using a pulse shaper (1800 L/mm pulse compression grating, Spectrogon; cylindrical lens with 200 mm focal length), normally 4.5 cm^{-1} fwhm and 7.5 mW in our experiments. The IR and VIS pulses were temporally and spatially overlapped on the $\text{TiO}_2(110)$ surface to generate SFG signal. The reflected broadband SFG signal was dispersed by a monochromator and then detected by an electron-multiplying CCD (Princeton Instrument). The incident angles of SFG, VIS, and IR were 47.9°, 45°, and 57°, respectively. Both polarizations of the VIS and IR were controlled by true zero-order half-wave plates, and the SFG signal polarization was selected and controlled by the combination of an achromatic half-wave plate and a Glan polarizer. The measured SFG spectra were normalized to the SFG signal of PPP polarization combination on the bare $\text{TiO}_2(110)$ surface obtained by flashing the sample to 700 K in UHV.

All DFT calculations were performed with generalized gradient approximation (GGA) of Perdew, Burke, and Ernzerhof (PBE) exchange-correlation functional⁶³ in the CP2K/QUICKSTEP⁶⁴ package. Valence electrons were described with a basis set at the double- ζ level, and core electrons were described with Goedecker–Teter–Hutter pseudopotentials.⁶⁵ A periodical slab of four TiO_2 trilayers with a 20 Å vacuum layer in z direction, defect-free 4×2 (11.836 Å × 12.994 Å) rutile $\text{TiO}_2(110)$ surface was employed. The slab is comprised of 64 TiO_2 units and all the atoms are relaxed. We have also checked the influence of the slab thickness to the adsorption energy, four-layer substrate is thick enough to represent the methanol state in the current study. (see Supporting Information) The cutoff energy for the plane-wave basis set is 320 Rybergs. Relaxation for atoms was carried out until the maximum residual force was less than 0.01 eV/Å. To get reasonable results, Hubbard U correction was also applied to Ti 3d orbitals and the U energy was set to 4.2 eV.^{56,66} We have also checked the influence of the U value at 3 and 5 eV, the relative energies between molecular and dissociated methanol are closed to that with U value at 4.2 eV (see Supporting Information). A constraint approach was also used to estimate the dissociation barrier of methanol. To describe the reaction's potential energy, the distances of the H and the O atom involved in the dissociation were used as the reaction coordinate, where the H is from the methanol molecule and the O can be the surface bridge oxygen or from the methanol in second layer. The energy profiles were obtained by varying the distances of H and O atoms involved in the dissociation. The adsorption energy E_a was obtained as

$$E_a = -1/n[E_{n\text{CH}_3\text{OH}/\text{TiO}_2} - (E_{\text{TiO}_2} + nE_{\text{CH}_3\text{OH}})] \quad (1)$$

where E_{TiO_2} , $E_{\text{CH}_3\text{OH}}$ and $E_{n\text{CH}_3\text{OH}/\text{TiO}_2}$ are the total energies of clean surface, free methanol, and the surface substrate with $n\text{CH}_3\text{OH}$, respectively. The n th adsorption energy E_a^n was obtained by as

$$E_a^n = -[E_{n\text{CH}_3\text{OH}/\text{TiO}_2} - (E_{(n-1)\text{CH}_3\text{OH}/\text{TiO}_2} + E_{\text{CH}_3\text{OH}})] \quad (2)$$

■ ASSOCIATED CONTENT

● Supporting Information

The Supporting Information is available free of charge on the ACS Publications website at DOI: [10.1021/acs.jpcllett.5b01417](https://doi.org/10.1021/acs.jpcllett.5b01417).

Fitting procedure of the SFG vibrational spectra. Figure S1: The visible and IR power-dependent SFG measurements of one layer methanol on TiO₂(110). Figure S2: Replotting the Figure 2 for clearer view of nonresonance. Figure S3: Replotting of the SFG spectra in Figure 4, with flashing temperature of 150 and 200 K to compare the peak at about 2890 cm⁻¹. Figure S4: Relation of the average methanol–surface distance and the *n*th adsorption energy to the methanol coverage. Figure S5: Top and side views of different adsorption configurations of 3/4 ML methanol in the first layer. Dashed lines represent hydrogen bonds. Figure S6: SFG *ssp* signal for ν_s vibrational modes of the CH₃ group against its polar angle. Table S1: The fitting results of SFG spectra in Figure 2. Table S2: The adsorption energies of different dissociated configurations in Figure S5. Table S3: Polar angles and azimuth angles of CH₃ group on the surface from the calculation results for one layer coverage. Influence of the slab thickness and U value on the relative energies between molecular and dissociated methanol on TiO₂(110). ([PDF](#))

■ AUTHOR INFORMATION

Corresponding Authors

*E-mail: limin.liu@csirc.ac.cn.

*E-mail: zfren@pku.edu.cn.

Author Contributions

[†]These authors contributed equally to this work.

Notes

The authors declare no competing financial interest.

■ ACKNOWLEDGMENTS

Z.R. thanks Timothy K. Minton from Montana State University for his helpful discussion. This work was supported by the National Basic Research Program of China (973 Program) under grant no. 2013CB834605; the National Natural Science Foundation of China under grant no. 1127002, 21322310, 5122212, 11290162, and 21403007; and Natural Science Foundation of Beijing under grant no. 2131002.

■ REFERENCES

- (1) Linsebigler, A. L.; Lu, G. Q.; Yates, J. T. Photocatalysis on TiO₂ Surfaces - Principles, Mechanisms, and Selective Result. *Chem. Rev.* **1995**, *95*, 735–758.
- (2) Diebold, U. The Surface Science of Titanium Dioxide. *Surf. Sci. Rep.* **2003**, *48*, 53–229.
- (3) Henderson, M. A. A Surface Science Perspective on Photocatalysis. *Surf. Sci. Rep.* **2011**, *66*, 185–297.
- (4) Mori, K.; Yamashita, H.; Anpo, M. Photocatalytic Reduction of CO₂ with H₂O on Various Titanium Oxide Photocatalysts. *RSC Adv.* **2012**, *2*, 3165–3172.
- (5) Lang, X.; Ma, W.; Chen, C.; Ji, H.; Zhao, J. Selective Aerobic Oxidation Mediated by TiO₂ Photocatalysis. *Acc. Chem. Res.* **2013**, *47*, 355–363.
- (6) Fujishima, A.; Honda, K. Electrochemical Photolysis of Water at a Semiconductor Electrode. *Nature* **1972**, *238*, 37–38.
- (7) Kawai, T.; Sakata, T. Photocatalytic Hydrogen Production from Liquid Methanol and Water. *J. Chem. Soc., Chem. Commun.* **1980**, 694–695.
- (8) Dohnálek, Z.; Lyubinetsky, I.; Rousseau, R. Thermally-driven Processes on Rutile TiO₂(110)-(1 × 1): A Direct View at the Atomic Scale. *Prog. Surf. Sci.* **2010**, *85*, 161–205.
- (9) Henderson, M. A.; Lyubinetsky, I. Molecular-Level Insights into Photocatalysis from Scanning Probe Microscopy Studies on TiO₂(110). *Chem. Rev.* **2013**, *113*, 4428–4455.
- (10) Henderson, M. A.; Otero-Tapia, S.; Castro, M. E. Electron-induced Decomposition of Methanol on the Vacuum-annealed Surface of TiO₂(110). *Surf. Sci.* **1998**, *412–413*, 252–272.
- (11) Wang, L.-Q.; Ferris, K. F.; Winokur, J. P.; Shultz, A. N.; Baer, D. R.; Engelhard, M. H. Interactions of Methanol with Stoichiometric and Defective TiO₂(110) and (100) Surfaces. *J. Vac. Sci. Technol., A* **1998**, *16*, 3034–3040.
- (12) A. Henderson, M.; Otero-Tapia, S.; E. Castro, M. The Chemistry of Methanol on the TiO₂(110) Surface: the Influence of Vacancies and Coadsorbed Species. *Faraday Discuss.* **1999**, *114*, 313–329.
- (13) Wong, G. S.; Kragten, D. D.; Vohs, J. M. The Oxidation of Methanol to Formaldehyde on TiO₂(110)-Supported Vanadia Films. *J. Phys. Chem. B* **2001**, *105*, 1366–1373.
- (14) Farfan-Arribas, E.; Madix, R. J. Role of Defects in the Adsorption of Aliphatic Alcohols on the TiO₂(110) Surface. *J. Phys. Chem. B* **2002**, *106*, 10680–10692.
- (15) Farfan-Arribas, E.; Madix, R. J. Different Binding Sites for Methanol Dehydrogenation and Deoxygenation on Stoichiometric and Defective TiO₂(110) Surfaces. *Surf. Sci.* **2003**, *544*, 241–260.
- (16) Onda, K.; Li, B.; Zhao, J.; Petek, H. The Electronic Structure of Methanol Covered TiO₂(110) Surfaces. *Surf. Sci.* **2005**, *593*, 32–37.
- (17) Zhang, Z. R.; Bondarchuk, O.; White, J. M.; Kay, B. D.; Dohnálek, Z. Imaging Adsorbate O-H Bond Cleavage: Methanol on TiO₂(110). *J. Am. Chem. Soc.* **2006**, *128*, 4198–4199.
- (18) Zhou, C.; Ren, Z.; Tan, S.; Ma, Z.; Mao, X.; Dai, D.; Fan, H.; Yang, X.; LaRue, J.; Cooper, R.; Wodtke, A. M.; Wang, Z.; Li, Z.; Wang, B.; Yang, J.; Hou, J. Site-specific Photocatalytic Splitting of Methanol on TiO₂(110). *Chem. Sci.* **2010**, *1*, 575–580.
- (19) Li, Z.; Smith, R. S.; Kay, B. D.; Dohnálek, Z. Determination of Absolute Coverages for Small Aliphatic Alcohols on TiO₂(110). *J. Phys. Chem. C* **2011**, *115*, 22534–22539.
- (20) Shen, M.; Henderson, M. A. Identification of the Active Species in Photochemical Hole Scavenging Reactions of Methanol on TiO₂. *J. Phys. Chem. Lett.* **2011**, *2*, 2707–2710.
- (21) Zhou, C.; Ma, Z.; Ren, Z.; Mao, X.; Dai, D.; Yang, X. Effect of Defects on Photocatalytic Dissociation of Methanol on TiO₂(110). *Chem. Sci.* **2011**, *2*, 1980–1983.
- (22) Phillips, K. R.; Jensen, S. C.; Baron, M.; Li, S.-C.; Friend, C. M. Sequential Photo-oxidation of Methanol to Methyl Formate on TiO₂(110). *J. Am. Chem. Soc.* **2013**, *135*, 574–577.
- (23) Yuan, Q.; Wu, Z.; Jin, Y.; Xu, L.; Xiong, F.; Ma, Y.; Huang, W. Photocatalytic Cross-Coupling of Methanol and Formaldehyde on a Rutile TiO₂(110) Surface. *J. Am. Chem. Soc.* **2013**, *135*, 5212–5219.
- (24) Bates, S. P.; Gillan, M. J.; Kresse, G. Adsorption of Methanol on TiO₂(110): A First-principles Investigation. *J. Phys. Chem. B* **1998**, *102*, 2017–2026.
- (25) Bates, S. P.; Kresse, G.; Gillan, M. J. The Adsorption and Dissociation of ROH Molecules on TiO₂(110). *Surf. Sci.* **1998**, *409*, 336–349.
- (26) Sanchez de Armas, R.; Oviedo, J.; San Miguel, M. A.; Sanz, J. F. Methanol Adsorption and Dissociation on TiO₂(110) from First Principles Calculations. *J. Phys. Chem. C* **2007**, *111*, 10023–10028.
- (27) Oviedo, J.; Sánchez-de-Armas, R.; San Miguel, M. A.; Sanz, J. F. Methanol and Water Dissociation on TiO₂(110): The Role of Surface Oxygen. *J. Phys. Chem. C* **2008**, *112*, 17737–17740.
- (28) Zhao, J.; Yang, J.; Petek, H. Theoretical Study of the Molecular and Electronic Structure of Methanol on a TiO₂(110) Surface. *Phys. Rev. B: Condens. Matter Mater. Phys.* **2009**, *80*, 235416.
- (29) Lang, X. F.; Wen, B.; Zhou, C. Y.; Ren, Z. F.; Liu, L. M. First-Principles Study of Methanol Oxidation into Methyl Formate on Rutile TiO₂(110). *J. Phys. Chem. C* **2014**, *118*, 19859–19868.

- (30) Migani, A.; Mowbray, D. J.; Iacomin, A.; Zhao, J.; Petek, H.; Rubio, A. Level Alignment of a Prototypical Photocatalytic System: Methanol on TiO₂(110). *J. Am. Chem. Soc.* **2013**, *135*, 11429–11432.
- (31) Shen, M.; Acharya, D. P.; Dohnálek, Z.; Henderson, M. A. Importance of Diffusion in Methanol Photochemistry on TiO₂(110). *J. Phys. Chem. C* **2012**, *116*, 25465–25469.
- (32) Shen, M.; Henderson, M. A. Role of Water in Methanol Photochemistry on Rutile TiO₂(110). *J. Phys. Chem. C* **2012**, *116*, 18788–18795.
- (33) Guo, Q.; Xu, C.; Ren, Z.; Yang, W.; Ma, Z.; Dai, D.; Fan, H.; Minton, T. K.; Yang, X. Stepwise Photocatalytic Dissociation of Methanol and Water on TiO₂(110). *J. Am. Chem. Soc.* **2012**, *134*, 13366–13373.
- (34) Guo, Q.; Xu, C.; Yang, W.; Ren, Z.; Ma, Z.; Dai, D.; Minton, T. K.; Yang, X. Methyl Formate Production on TiO₂(110), Initiated by Methanol Photocatalysis at 400 nm. *J. Phys. Chem. C* **2013**, *117*, S293–S300.
- (35) Xu, C.; Yang, W.; Ren, Z.; Dai, D.; Guo, Q.; Minton, T. K.; Yang, X. Strong Photon Energy Dependence of the Photocatalytic Dissociation Rate of Methanol on TiO₂(110). *J. Am. Chem. Soc.* **2013**, *135*, 19039–19045.
- (36) Xu, C.; Yang, W.; Guo, Q.; Dai, D.; Chen, M.; Yang, X. Molecular Hydrogen Formation from Photocatalysis of Methanol on TiO₂(110). *J. Am. Chem. Soc.* **2013**, *135*, 10206–10209.
- (37) Mao, X.; Wei, D.; Wang, Z.; Jin, X.; Hao, Q.; Ren, Z.; Dai, D.; Ma, Z.; Zhou, C.; Yang, X. Recombination of Formaldehyde and Hydrogen Atoms on TiO₂(110). *J. Phys. Chem. C* **2015**, *119*, 1170–1174.
- (38) Chabal, Y. J. Surface Infrared-Spectroscopy. *Surf. Sci. Rep.* **1988**, *8*, 211–357.
- (39) Xu, M.; Gao, Y.; Wang, Y.; Woell, C. Monitoring Electronic Structure Changes of TiO₂(110) via Sign Reversal of Adsorbate Vibrational Bands. *Phys. Chem. Chem. Phys.* **2010**, *12*, 3649–3652.
- (40) Wang, Y.; Wöll, C. Chemical Reactions on Metal Oxide Surfaces Investigated by Vibrational Spectroscopy. *Surf. Sci.* **2009**, *603*, 1589–1599.
- (41) Shen, Y. R. Surface-properties Probed by 2nd-harmonic and Sum-frequency Generation. *Nature* **1989**, *337*, 519–525.
- (42) Tian, C. S.; Shen, Y. R. Recent Progress on Sum-frequency Spectroscopy. *Surf. Sci. Rep.* **2014**, *69*, 105–131.
- (43) Wang, H.-F.; Velarde, L.; Gan, W.; Fu, L. Quantitative Sum-Frequency Generation Vibrational Spectroscopy of Molecular Surfaces and Interfaces: Lineshape, Polarization, and Orientation. *Annu. Rev. Phys. Chem.* **2015**, *66*, 189–216.
- (44) Wu, W.-C.; Chuang, C.-C.; Lin, J.-L. Bonding Geometry and Reactivity of Methoxy and Ethoxy Groups Adsorbed on Powdered TiO₂. *J. Phys. Chem. B* **2000**, *104*, 8719–8724.
- (45) Panayotov, D. A.; Burrows, S. P.; Morris, J. R. Photooxidation Mechanism of Methanol on Rutile TiO₂ Nanoparticles. *J. Phys. Chem. C* **2012**, *116*, 6623–6635.
- (46) Wang, C.-Y.; Groenzin, H.; Shultz, M. J. Surface Characterization of Nanoscale TiO₂ Film by Sum Frequency Generation Using Methanol as a Molecular Probe. *J. Phys. Chem. B* **2004**, *108*, 265–272.
- (47) Feng, R.-r.; Liu, A.-a.; Liu, S.; Shi, J.; Zhang, R.; Ren, Z. In Situ Studies on the Dissociation and Photocatalytic Reactions of CH₃OH on TiO₂ Thin Film by Sum Frequency Generation Vibrational Spectroscopy. *J. Phys. Chem. C* **2015**, *119*, 9798–9804.
- (48) Superfine, R.; Huang, J. Y.; Shen, Y. R. Nonlinear Optical Studies of the Pure Liquid/Vapor Interface: Vibrational Spectra and Polar Ordering. *Phys. Rev. Lett.* **1991**, *66*, 1066–1069.
- (49) Lu, R.; Gan, W.; Wu, B.-H.; Zhang, Z.; Guo, Y.; Wang, H.-F. C–H Stretching Vibrations of Methyl, Methylene and Methine Groups at the Vapor/Alcohol (n = 1–8) Interfaces. *J. Phys. Chem. B* **2005**, *109*, 14118–14129.
- (50) Jang, J. H.; Lydiatt, F.; Lindsay, R.; Baldelli, S. Quantitative Orientation Analysis by Sum Frequency Generation in the Presence of Near-Resonant Background Signal: Acetonitrile on Rutile TiO₂ (110). *J. Phys. Chem. A* **2013**, *117*, 6288–6302.
- (51) Gálvez, Ó.; Maté, B.; Martín-Llorente, B.; Herrero, V. J.; Escrivano, R. Phases of Solid Methanol. *J. Phys. Chem. A* **2009**, *113*, 3321–3329.
- (52) Snyder, R. G.; Scherer, J. R. Band Structure in the C–H Stretching Region of the Raman Spectrum of the Extended Polymethylene Chain: Influence of Fermi Resonance. *J. Chem. Phys.* **1979**, *71*, 3221–3228.
- (53) Snyder, R. G.; Strauss, H. L.; Elliger, C. A. Carbon-hydrogen Stretching Modes and the Structure of n-alkyl Chains. 1. Long, Disordered Chains. *J. Phys. Chem.* **1982**, *86*, 5145–5150.
- (54) Snyder, R. G.; Aljibury, A. L.; Strauss, H. L.; Casal, H. L.; Gough, K. M.; Murphy, W. F. Isolated C–H Stretching Vibrations of n-alkanes: Assignments and Relation to Structure. *J. Chem. Phys.* **1984**, *81*, 5352–5361.
- (55) Liu, L.-M.; Zhang, C.; Thornton, G.; Michaelides, A. Structure and dynamics of liquid water on rutile TiO₂. *Phys. Rev. B: Condens. Matter Mater. Phys.* **2010**, *82*, 161415.
- (56) Sun, C.; Liu, L.-M.; Selloni, A.; Lu, G. Q.; Smith, S. C. Titania-water interactions: a review of theoretical studies. *J. Mater. Chem.* **2010**, *20*, 10319–10334.
- (57) Wang, R.; Fan, H. The Adsorption and Dissociation of Multilayer CH₃OH on TiO₂ (110). *Sci. China: Chem.* **2015**, *58*, 614–619.
- (58) Kimmel, G. A.; Baer, M.; Petrik, N. G.; VandeVondele, J.; Rousseau, R.; Mundy, C. J. Polarization- and Azimuth-Resolved Infrared Spectroscopy of Water on TiO₂(110): Anisotropy and the Hydrogen-Bonding Network. *J. Phys. Chem. Lett.* **2012**, *3*, 778–784.
- (59) Haubrich, J.; Kaxiras, E.; Friend, C. M. The Role of Surface and Subsurface Point Defects for Chemical Model Studies on TiO₂: A First-Principles Theoretical Study of Formaldehyde Bonding on Rutile TiO₂(110). *Chem. - Eur. J.* **2011**, *17*, 4496–4506.
- (60) Wang, H. F.; Gan, W.; Lu, R.; Rao, Y.; Wu, B. H. Quantitative spectral and orientational analysis in surface sum frequency generation vibrational spectroscopy (SFG-VS). *Int. Rev. Phys. Chem.* **2005**, *24*, 191–256.
- (61) Liu, A.-A.; Liu, S.; Zhang, R.; Ren, Z. Spectral Identification of Methanol on TiO₂(110) Surfaces with Sum Frequency Generation in the C–H Stretching Region, submitted for publication.
- (62) Liu, S.; Liu, A.-A.; Zhang, R.; Ren, Z. Compact Ultrahigh Vacuum/High-pressure System for Broadband Infrared Sum Frequency Generation Vibrational Spectroscopy Studies, submitted for publication.
- (63) Perdew, J. P.; Burke, K.; Ernzerhof, M. Generalized Gradient Approximation Made Simple. *Phys. Rev. Lett.* **1996**, *77*, 3865–3868.
- (64) VandeVondele, J.; Krack, M.; Mohamed, F.; Parrinello, M.; Chassaing, T.; Hutter, J. Quickstep: Fast and Accurate Density Functional Calculations Using a Mixed Gaussian and Plane Waves Approach. *Comput. Phys. Commun.* **2005**, *167*, 103–128.
- (65) Goedecker, S.; Teter, M.; Hutter, J. Separable Dual-space Gaussian Pseudopotentials. *Phys. Rev. B: Condens. Matter Mater. Phys.* **1996**, *54*, 1703–1710.
- (66) Morgan, B. J.; Watson, G. W. A DFT+U Description of Oxygen Vacancies at the TiO₂ Rutile (110) Surface. *Surf. Sci.* **2007**, *601*, 5034–5041.